Micro-Newton Electrospray Thrusters for China's Space-Borne Gravitational Wave Detection Mission (TianQin)

IEPC-2019- A-284

Presented at the 36th International Electric Propulsion Conference
University of Vienna • Vienna, Austria
September 15-20, 2019

Peiyi Song[1, *], Leimeng Sun[1, *], Shuangyang Kuang[1], Kai Zhang[1], Wentao Zou[1], Xiaochen Suo[1], Yurong Wang[1], Dongyang Xiao[1], Liang-Cheng Tu[1, 2, *]

[1] *MOE Key Laboratory of Fundamental Physical Quantities Measurement & Hubei Key Laboratory of Gravitation and Quantum Physics, PGMF and School of Physics, Huazhong University of Science and Technology, Wuhan 430074, P. R. China.*
[2] *TianQin Research Center for Gravitational Physics, School of Physics and Astronomy, Sun Yat-sen University, Zhuhai, 519082, China*

* *Corresponding Author SONGPEIYI@hust.edu.cn, SUNLEIMENG@hust.edu.cn and TLC@hust.edu.cn;*

Abstract: In this paper, a MEMS-based micro-newton electrospray thruster for space borne gravitational wave detection mission is discussed. We present the design philosophy, key components, thrust control methodologies, fabrication and characterization methods of the thruster. The thruster provides forces by propulsion of charged particles that are emitted from ionic liquid through field emission and accelerated in an electrostatic field. To achieve such a small thrust required by the mission, the emitter is made into micron-size to allow an extremely small flow rate (< 1nL/min) of propellant being ionized and emitted. In our approach, the flow rate is achieved on ultra-small diameter capillaries which provide very high flow impedance as well as a confined space of emission. The capillary emitter is fabricated on a silicon-on-insulator (SOI) wafer through inductive coupled plasma etching (ICP) and reactive ion etching (RIE). Emitters with the inner diameters less than 10 μm are fabricated. 0.1 μN thrust resolution is realized by precise controls of three parameters: the propellant's flow rate, the acceleration voltage as well as the number of working emitters. For this approach, we design a MEMS high-resolution proportional valve with

piezoelectric actuation as the flow rate regulator. A high precision capacitance displacement sensor is integrated onto the valve membrane to monitor the position of valve membrane real time in order to develop a close-loop control for reducing flow rates fluctuations. Selectively switching on a certain number of emitters is achieved through digital control of the emitters array. Last but not the least, a MEMS neutralizer is being developed based on cold-field-emission over carbon nanotubes (CNTs) grown on a silicon substrate to emit pure electrons. The thruster system features compact size, high resolution and modular operation capabilities, offering superior robustness and consistency.

I. Introduction

CURRENT efforts aiming at direct detection of gravitational waves (GWs) include several ongoing laser interferometer projects on the ground, such as Laser Interferometer Gravitational-Wave Observatory (LIGO), and space-borne programs such as Laser Interferometer Space Antenna (LISA)[1], DECIGO [2], China's Taiji[3] and TianQin[4] project. TianQin is a space-borne experiment, which aims to detect gravitational waves in the millihertz (mHz) range (i.e. 0.1–100 mHz)[4]. GWs in this frequency range could come from a plethora of important astronomical sources, such as ultra-compact galactic binaries, coalescing massive black holes, and the capture of stellar objects by massive black holes, making the detection of them to be of great significance[5-7]. The experiment relies on a constellation of three spacecraft orbiting the earth. Inter-spacecraft laser interferometry is used to monitor the displacement between test masses, with the precision of 10^{-12} m/√Hz. The experiment is designed to be capable of detecting a signal with high confidence from a single source of gravitational waves within a few months of observing time. To enable the detection with high precisions, each spacecraft is working in drag-free mode that will have a disturbance reduction system (DRS) to reduce the effects of the non-gravitational forces on the test masses (which are the reference points for the laser interferometer)[8-9]. Thruster is one of the key part of the DRS, which provides actuation forces to balance non-gravitational forces over the spacecraft. Such forces are estimated to be in micro-newton level, measured by the inertial sensors on the satellite in real-time[10].

Propulsion technologies that could meet TianQin's requirements include micro-newton level cold-gas thrusters[11] and electric propulsion thrusters[12]. As comparison, cold-gas propulsion is a well-developed technology, showing stable, robust and consistent performance than others. However, the bulky and complex system as well as its relatively small specific impulsion make the using of cold-gas propulsion in long-term detection mission much more challenging. Electric propulsion, on the other hand, featuring higher specific impulsion and lesser system complexity. Another outstanding advantage of electric propulsion for the GWs detection mission is that the thrust can be controlled automatically in a close-loop, which contributes to the increasing of thrust resolution and the reducing of noises[13]. To date, several micro-newton electric thrusters are developed, including the field emission electrospray thrusters (FEEP)[14] that use liquid metal as the propellant, the colloid micro-newton thrusters (CMNT)[15] that use ionic liquid as the propellant and plasma thrusters that use inert gas as the propellant[16]. BUSEK has demonstrated the in-flight test of both cold-gas thrusters and CMNTs, measurements indicate that the micro-newton electrospray propulsion thruster has met requirements of LISA and it exhibits lower noise level than cold-gas thrusters[13]. Electrospray propulsion thruster is definitely a promising candidate for

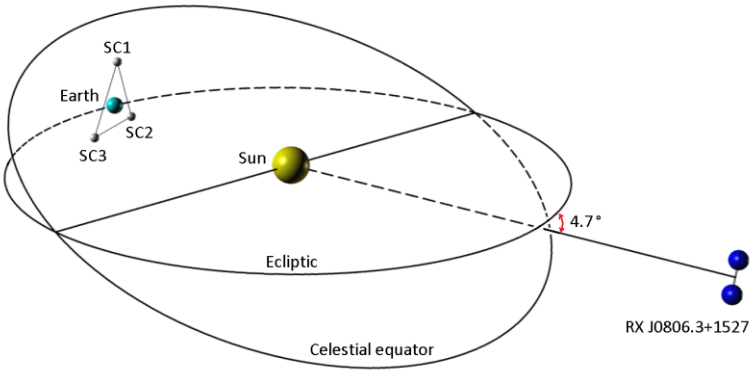

Figure 1. An illustration of the preliminary concept of TianQin, with J0806 being the reference source. The three TianQin spacecraft are denoted as SC1, SC2 and SC3. The plane of the celestial equator is also shown, together with the direction to J0806 in the sky.

future GWs detection missions, but few major problems are awaiting solutions. First, continuous working of the thruster brings unavoidable damages and contaminations onto emitters and electrodes, which significantly affect the thrust performance and lifetime[17-18]. Second, the minimum and maximum thrust are controlled by the field emission voltages, which are restricted in a small range to avoid emission instabilities, offering limited ability in thrust control. Lastly, the system size and weight shall be further reduced to enable the integration of more thrusters into one system, adding more degrees of freedom for the operation, as well as more backups (redundancy) for DRS.

In this paper, a MEMS-based micro-newton electrospray thruster for in-planning space borne GWs detection mission is discussed. We present the design philosophy, key components, control methodologies, fabrication processes and characterization methods of the thruster. Based on our calculation, the thrusters for the TianQin's drag-free satellites should be able to provide a continuous thrust from 1 micro-newton (μN) to 30 μN with the controllable resolution of 0.1 μN, the thrust noise below 0.1 μN/Hz$^{1/2}$, the response time less than 200 milliseconds (ms) and the total lifetime longer than 10000 hours.

II. Design Philosophy

We aim to develop a thruster that is able to provide micro-newton level thrust with high resolution, in the same time find solutions for the current technical challenges. In this work, a microelectromechanical systems (MEMS) based field emission electrospray thruster is proposed. First, in order to achieve such a small thrust, emitters of this thruster shall be made as small as possible to allow very small amount of propellant being ionized and emitted. As the propellant is liquid, a capillary emitter with ultra-small inner diameter is designed to provide the low flow rate as well as the confined field emission space. Based on current MEMS technologies, emitters with the inner diameters less than 10 μm can be fabricated. The emitter is fabricated using a silicon-on-insulator (SOI) wafer through inductive coupled plasma etching (ICP) and reactive ion etching (RIE), which are all commonly used processes in MEMS. Second, in order to achieve the high-resolution thrust control, propellant's feeding flow rate shall be regulated with high resolution too. The flow rates can be even less than 1 nL/min[19]. Microfluidics, a technology originated from MEMS, is considered to be applied for this purpose, Microfluidics is a technology for developing devices with micro-channels, micro-valves and micro-actuators to accurately control the flowing liquid. However, the wide thrust range needed in the GW detection mission means that either the flow rate or the field emission voltage must be modified dramatically, which may introduce cone-jet instabilities into the electrospray thruster's operation. In our design, this challenge can be solved by adding more emitters into the operation. When a large thrust is requested, we can add the number of

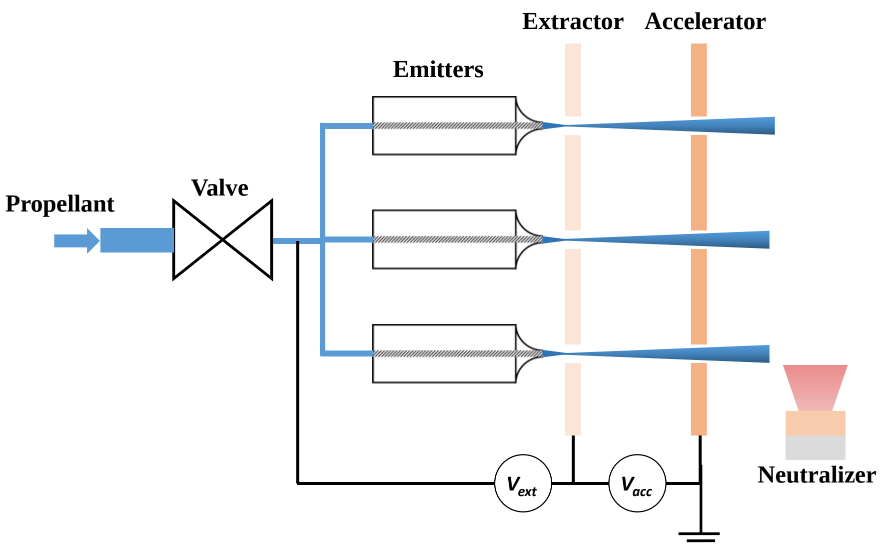

Figure 2. Schematic of the thruster's working mechanism.

working emitters to provide a total thrust and make sure each emitter is operated in a stable condition. Obviously, an emitters array must be equipped in the thruster to guarantee the control precision. It is worth mentioning that, it is possible to fabricate the emitters array on silicon substrate through standard MEMS fabrication with high uniformity. Interesting noting that, selectively switching on a certain number of emitters not only provide thrust control, but also allows one part of emitters to rest or recover while providing the continuous thrust, which can significantly reduce the damage and contamination over emitters and electrodes, eventually contributing to a longer lifetime and better thrust consistency.

This can be achieved through digital operation over the emitters array, which is another advantage of adopting MEMS technology since many MEMS devices have been enabled with digital working capabilities.

III. Thruster System

The field emission electrospray thruster has four major parts: 1. Capillary emitters array; 2. Neutralizer or cathode; 3. Micro valve; 4. Power management unit (PMU) and temperature control unit (TCU). The schematic of the thruster is demonstrated in Figure 3.

Capillary Emitters Array

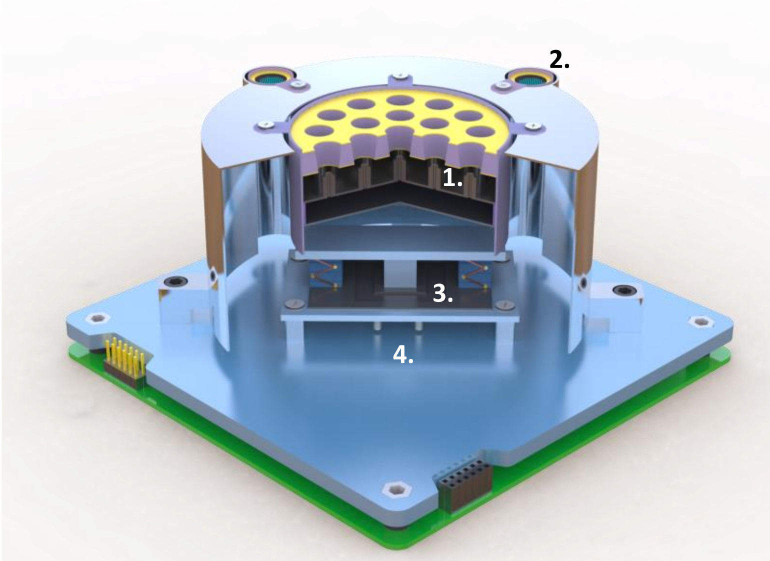

Figure 3. 3D drawing of the thruster.

The capillary emitters array is a chip-like component (Figure 4), fabricated on a SOI wafer. Each emitter has a capillary needle structure with the inner diameter of 5 μm, the outer diameter of 50 μm, the height of 100 μm and a sharpened tip. The long channel with small inner diameter contributes to the ultra-small flow rate of propellant. Propellant is feed into a reservoir and then flows into the capillary of

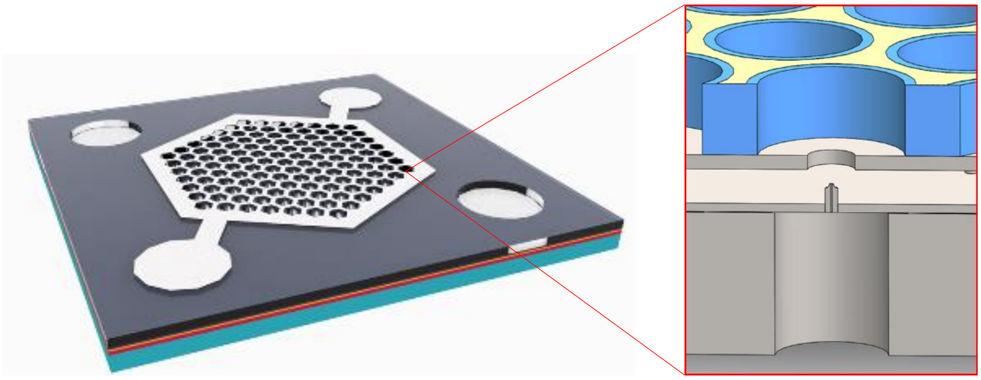

Figure 4. 3D drawing of the emitters chip.

each emitter. The sharpened emitter tip helps in lowering the onset voltage of Taylor cone, since the electrical field is amplified at the surface with smaller radius of curvature. On top of the emitters array, a glass wafer coated with gold is bonded serving as the electrodes (extractor and accelerator) for field emission and particles acceleration. A circular hole is drilled on the glass wafer for each emitter with the diameter of 100 μm and the deep of 250 μm.

Neutralizer

As shown in Figure 5, a carbon nanotubes (CNTs) array is used as the field emission (FE) material in the neutralizer. The neutralizer is constructed of three parts, including an electrons emitter, an insulating layer and a gate screen. CNTs array is grown on silicon substrate through a thermal chemical vapor deposition (TCVD) process. In this design, the CNTs array is peeled off from the growing silicon substrate and transferred to the target substrate with an improved bonding method to enhance the

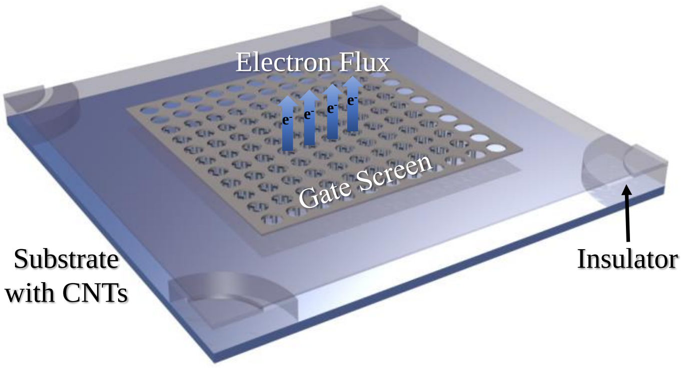

Figure5. CNTs field emission system as the neutralizer.

adhesion between CNTs array and substrate, which contributes to higher robustness. The target substrate has excellent thermal conductivity (aluminum nitride ceramic substrate). Before the transfer, we will grow a layer of graphene on the top of the CNT, and then deposit an alloy on the graphene and the target substrate for metal bonding. Compared with the traditional transfer method (directly transferring CNTs onto the target substrate), strong chemical bonds can be formed between the graphene and the CNTs. Also, thermal diffusion between CNTs and substrate are accelerated. When a proper electric field is applied between the gate electrode and the emission cathode, electrons will be extracted out from the CNTs and being emitted out of the gate to neutralize positive ions from the thruster emitters. Since CNTs have a high aspect ratio, the large electric field could be formed with a relatively low turn-on voltage for realizing the emission. Thus, the neutralizer features low power consumption as compared with traditional hollow cathodes. Another key parameter of the neutralizer to evaluate its efficiency is the electrons transmittance. In this study, we conduct a series of simulation works to find a design for the gate screen, in which the electrons transmittance is increased to be higher than 63%.

Piezoelectric Micro-Valve

The piezoelectric micro-valve is used to regulate the flow rate of propellant feeding into the emitters. The valve is actuated by piezoelectric materials (e.g. lead zirconate titanate, PZT) to induce displacements of the valve membrane, which determines the flow resistance of the valve's microchannel. With a fixed input pressure, we can then determine the output flow rate of the propellant. As the flow rate control resolution required is 1 nL/min, the displacement control resolution shall be better than 40 nm based on our design. Indeed, to increase the resolution and reduce noises, a displacement sensor is integrated onto the valve membrane, which is based on capacitance displacement sensing that is commonly used in MEMS inertial sensors. The sensor has two conductive plates with one attaching on the moving membrane and another attaching on the fixed side wall. Displacement less than 1 nm can be detected by the sensor, which meets the requirement for this valve. In this way, we can also design a close-loop control for this valve's high resolution operation and in the mean while reduce noises from the piezoelectric actuation.

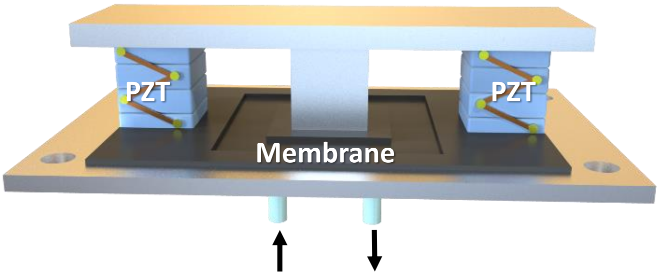

Figure 6. 3D drawing of the piezoelectric micro-valve.

Power Management Unit and Temperature Control Unit

The PMU contains high voltage DC-DC converters, provides power and digital controls for emitters, neutralizers, valves and TCU. The TCU is used for maintain a fixed temperature at the emitter, especially the temperature of the propellant. The TCU includes temperature sensors, heaters and electronics, which is all integrated into one unit and placed at the back of emitters chip. Thruster's electronics are controlled with a digital microcontroller.

IV. Thrust Control Methodology

The control of thrust is achieved through the real-time adjustment of multiple parameters, including the heater voltage V_h that determines the propellant's temperature, the valve voltage V_v that controls the flow rates, the emitter voltage V_e and extractor voltage V_{ex} that determine the establishment of field emission, the accelerator voltage V_{ac} that determines jet's speed, and the CNTs emission voltage V_{ne} that controls the cathode's currents (Figure 7a). In the operation, the temperature T, valve membrane's displacement sensing voltage V_{cp} and emitter's current I_e are measured for the close-loop control of thrust, the cathode currents I_{ne} shall match with the I_e. Propellant is kept at a fixed temperature. Upon a thrust command, V_e and V_{ex} are quickly adjusted to give a fast change of thrust, following with changing V_v to match the need for propellant rate. Our software simulation indicates that the 0.1 μN thrust resolution and response time less than 300 ms can be achieved based on this control methodology (Figure 7b). If

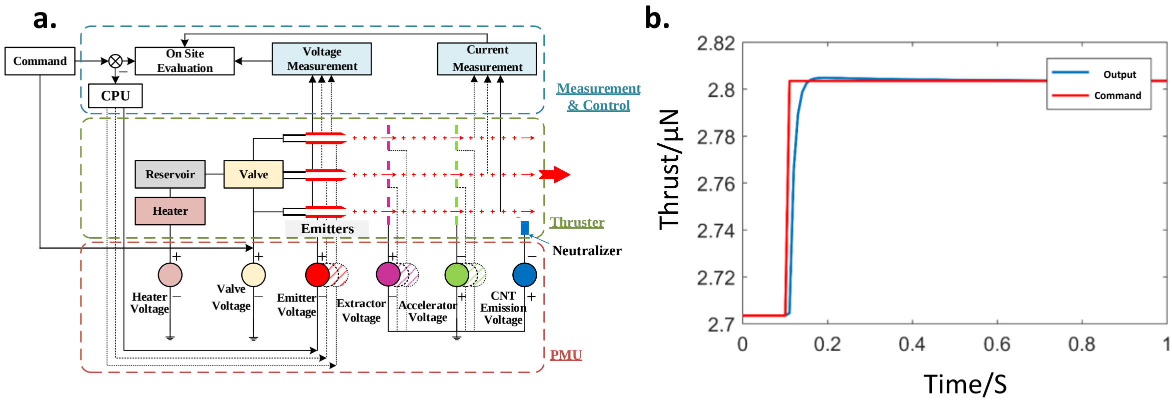

Figure 7. a. Thruster electrical schematic and control methodology. b. Software simulation of thrust control over 0.1 μN thrust increment.

the thrust changes in a large scale, instead of dramatically changing voltages, we increase/reduce the number of emitters N_e to meet the total thrust in order to avoid instabilities of field emission under very high/low voltages. Moreover, even though the thruster is operated in continuous thrust mode, we can choose one part of emitters in working and set the others in a reverse-voltage mode for reducing the contamination of charged ions and damage of emitter structures in the continuously emission.

V. Fabrication and Integration

The fabrication of capillary emitters array is through standard MEMS processes on a SOI wafer, including photolithography, inductively coupled plasma (ICP) dry etching and reactive-ion etching (RIE) to form the capillary and reservoir structure. The capillary internal diameter less than 10 μm is achieved (Figure 8). The field emission electrodes structure is deposited on a glass wafer through electron beam (E-beam) deposition, holes on a 100 μm thickness glass wafer is achieved through laser micromachining with the diameter of 100 μm. The processed SOI wafer and glass wafer are bonded with an insulator layer (PET or Silicon Dioxide) of 80-100 μm. Other structures are fabricated by precision machining on metals as well as 3D printing.

VI. Characterization Method

In the early development of the thruster, we build a time-of-flight (TOF) system for preliminary characterization of the thrust, specific impulse and jet components, which is a commonly used technique in other studies[20]. For accurately measuring the thrust range, resolution, response time and noise, two precision measurement systems are developed including a torsion system for the characterization of static features and a pendulum system for dynamic characterizations. The noise level of these systems are measured and shown in figure 9, which are lower than the requirement (0.1 $\mu N/Hz^{1/2}$) on the required frequencies.

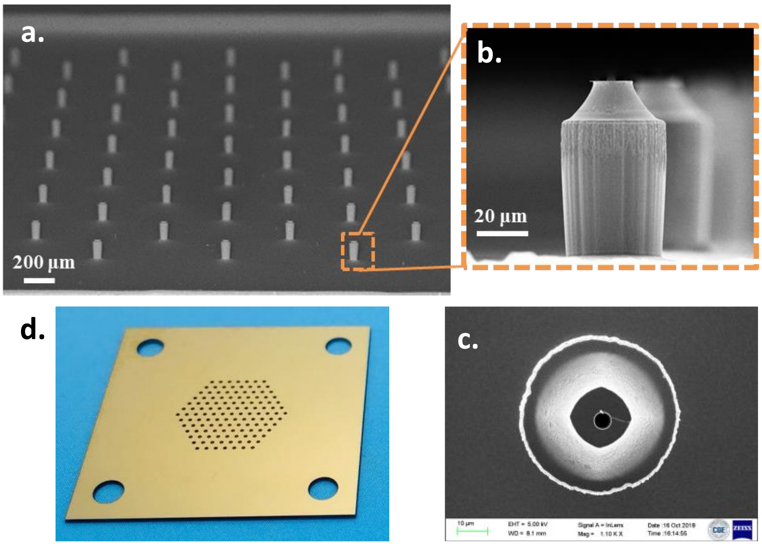

Figure 8. a. SEM image of fabricated emitters array. b. SEM image of one emitter with sharpened tip. c. SEM top view image of the capillary emitter. d. Gold deposited glass wafer with laser micro-machined structure.

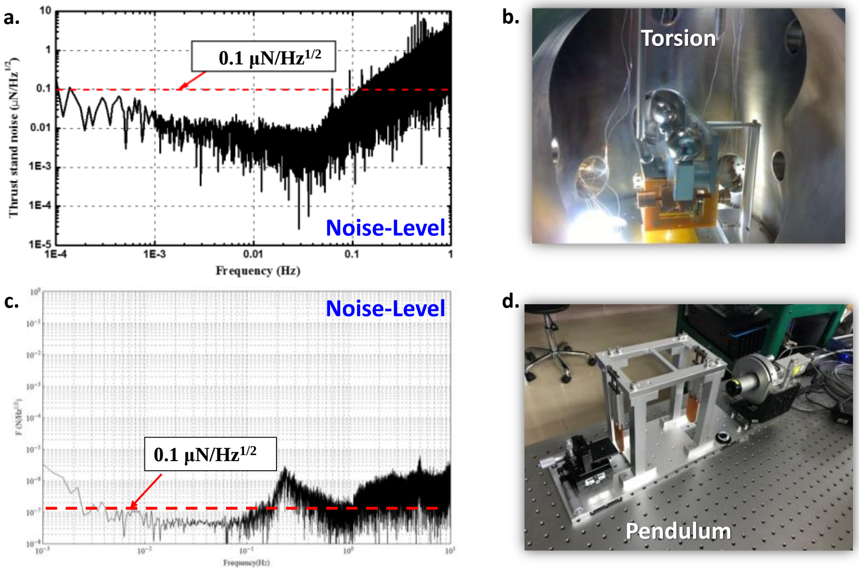

Figure 9. a. Noise level of the torsion thrust characterization system as the function of frequency. b. Photography of the torsion system. c. Noise level of the thrust characterization pendulum system as the function of frequency. d. Photograph of the pendulum system.

VII. Summary and Future Plan

In summary, a MEMS-based micro-newton level field emission electrospray thruster is designed for China's space borne GW detection mission. The thruster contains a capillary emitters array which is able to provide small thrust as well as multiple modes for stable operation. By adding/reducing the number of emitters, we gain a way to modify the thrust without dramatically changing the voltages. By using parts of emitters in one time and let other emitters rest or recover, we find a practical way to increase a single emitter's lifetime thus the thruster's robustness is lifted. Based on this design, thrust control methodologies are discussed to enable the 0.1 μN resolution and response time less than 300 ms. At last, the fabrication and characterization methods are discussed in this paper. Our future plan is to complete the thruster system and conduct basic characterizations using ground facilities in the next five years. Over the next stage, we will look for in-flight test opportunities to test the principle prototypes in one DRS loop.

Acknowledgments

This work is supported by National Natural Science Foundation of China (NSFC 11927812), Startup Grant of Huazhong University of Science and Technology and Development Grant of Sun Yat-Sen University. The authors would like to acknowledge the contributions of HIT Institute of Advanced Power and TianQin Research Center for Gravitational Physics.

References

1. Audley, H.; Babak, S.; Baker, J.; Barausse, E.; Bender, P.; Berti, E.; Binetruy, P.; Born, M.; Bortoluzzi, D.; Camp, J., Laser Interferometer Space Antenna. *Tp.umu.se* **2017,** *548* (3), 411.
2. Kawamura, S.; Nakamura, T.; Ando, M.; Seto, N.; Akutsu, T.; Funaki, I.; Ioka, K.; Kanda, N.; Kawano, I.; Musha, M., Space gravitational-wave antennas DECIGO and B-DECIGO. *International Journal of Modern Physics D* **2018**, 1845001.
3. Hu, W. R.; Wu, Y. L., The Taiji Program in Space for gravitational wave physics and the nature of gravity. *National Science Review* **2017,** (5), 685-686.
4. Luo, J.; Chen, L.-S.; Duan, H.-Z.; Gong, Y.-G.; Hu, S.; Ji, J.; Liu, Q.; Mei, J.; Milyukov, V.; Sazhin, M.; Shao, C.-G.; Toth, V. T.; Tu, H.-B.; Wang, Y.; Wang, Y.; Yeh, H.-C.; Zhan, M.-S.; Zhang, Y.; Zharov, V.; Zhou, Z.-B., TianQin: a space-borne gravitational wave detector. *Classical and Quantum Gravity* **2016,** *33* (3), 035010.
5. Abbott, B. P.; Abbott, R.; Abbott, T. D.; Acernese, F.; Ackley, K.; Adams, C.; Adams, T.; Addesso, P.; Adhikari, R. X.; Adya, V. B., GW170817: Observation of Gravitational Waves from a Binary Neutron Star Inspiral. *Physical Review Letters* **2017,** *119* (16), 161101.
6. Harry, G.; Fritschel, P.; Folkner, W.; Shaddock, D.; Sterl Phinney, E., *The Big Bang Observer: High Laser Power for Gravitational Wave Astrophysics*. 2007.
7. Takahashi, R.; Nakamura, T., The Decihertz Laser Interferometer Can Determine the Position of the Coalescing Binary Neutron Stars within an Arcminute a Week before the Final Merging Event to the Black Hole. *Astrophysical Journal* **2008,** *596* (2).
8. Lange, B., The Drag-Free Satellite. *Aiaa Journal* **2011,** *2* (9), 1590-1606.
9. Lange, B. In *Techniques for a High-Precision Frame-Dragging Measurement Using an Unsupported Gyroscope in a Drag-Free Satellite*, Recent Developments in Theoretical & Experimental General Relativity, Gravitation, & Relativistic Field Theories, 1999.
10. Gamero-Castaño, M.; Hruby, V.; Spence, D.; Demmons, N.; McCormick, R.; Gasdaska, C., *Micro Newton Colloid Thruster System Development for ST7-DRS Mission*. 2003.
11. Armano, M.; Audley, H.; Auger, G.; Baird, J.; Binetruy, P.; Born, M.; Bortoluzzi, D.; Brandt, N.; Bursi, A.; Caleno, M.; Cavalleri, A.; Cesarini, A.; Cruise, M.; Danzmann, K.;

Diepholz, I.; Dolesi, R.; Dunbar, N.; Ferraioli, L.; Ferroni, V.; Zweifel, P., *A Strategy to Characterize the LISA-Pathfinder Cold Gas Thruster System*. 2015; Vol. 610, p 012026.
12. Anderson, G.; Anderson, J.; Anderson, M.; Aveni, G.; Bame, D.; Barela, P.; Blackman, K.; Carmain, A.; Chen, L.; Cherng, M.; Clark, S.; Connally, M.; Connolly, W.; Conroy, D.; Cooper, M.; Cutler, C.; D'Agostino, J.; Demmons, N.; Dorantes, E.; Dunn, C.; Duran, M.; Ehrbar, E.; Evans, J.; Fernandez, J.; Franklin, G.; Girard, M.; Gorelik, J.; Hruby, V.; Hsu, O.; Jackson, D.; Javidnia, S.; Kern, D.; Knopp, M.; Kolasinski, R.; Kuo, C.; Le, T.; Li, I.; Liepack, O.; Littlefield, A.; Maghami, P.; Malik, S.; Markley, L.; Martin, R.; Marrese-Reading, C.; Mehta, J.; Mennela, J.; Miller, D.; Nguyen, D.; O'Donnell, J.; Parikh, R.; Plett, G.; Ramsey, T.; Randolph, T.; Rhodes, S.; Romero-Wolf, A.; Roy, T.; Ruiz, A.; Shaw, H.; Slutsky, J.; Spence, D.; Stocky, J.; Tallon, J.; Thorpe, I.; Tolman, W.; Umfress, H.; Valencia, R.; Valerio, C.; Warner, W.; Wellman, J.; Willis, P.; Ziemer, J.; Zwahlen, J.; Armano, M.; Audley, H.; Baird, J.; Binetruy, P.; Born, M.; Bortoluzzi, D.; Castelli, E.; Cavalleri, A.; Cesarini, A.; Cruise, A. M.; Danzmann, K.; de Deus Silva, M.; Diepholz, I.; Dixon, G.; Dolesi, R.; Ferraioli, L.; Ferroni, V.; Fitzsimons, E. D.; Freschi, M.; Gesa, L.; Gibert, F.; Giardini, D.; Giusteri, R.; Grimani, C.; Grzymisch, J.; Harrison, I.; Heinzel, G.; Hewitson, M.; Hollington, D.; Hoyland, D.; Hueller, M.; Inchauspé, H.; Jennrich, O.; Jetzer, P.; Karnesis, N.; Kaune, B.; Korsakova, N.; Killow, C. J.; Lobo, J. A.; Lloro, I.; Liu, L.; López-Zaragoza, J. P.; Maarschalkerweerd, R.; Mance, D.; Meshksar, N.; Martín, V.; Martin-Polo, L.; Martino, J.; Martin-Porqueras, F.; Mateos, I.; McNamara, P. W.; Mendes, J.; Mendes, L.; Nofrarias, M.; Paczkowski, S.; Perreur-Lloyd, M.; Petiteau, A.; Pivato, P.; Plagnol, E.; Ramos-Castro, J.; Reiche, J.; Robertson, D. I.; Rivas, F.; Russano, G.; Sopuerta, C. F.; Sumner, T.; Texier, D.; Vetrugno, D.; Vitale, S.; Wanner, G.; Ward, H.; Wass, P. J.; Weber, W. J.; Wissel, L.; Wittchen, A.; Zweifel, P., Experimental results from the ST7 mission on LISA Pathfinder. *Physical Review D* **2018,** *98* (10), 102005.
13. Armano, M.; Audley, H.; Baird, J.; Binetruy, P.; Born, M.; Bortoluzzi, D.; Castelli, E.; Cavalleri, A.; Cesarini, A.; Cruise, A., LISA Pathfinder micronewton cold gas thrusters: In-flight characterization. *Physical Review D* **2019,** *99* (12), 122003.
14. Nicolini, D.; Frigot, P.-E.; Musso, F.; Cesare, S.; Castorina, G.; Ceruti, L.; Bartola, F.; Zanella, P.; Ceccanti, F.; Priami, L.; Paita, L., *Direct Thrust and Thrust Noise Measurements on the LISA Pathfinder Field Emission Thruster*. 2019.
15. Hruby, V.; Spence, D.; Demmons, N.; Roy, T.; Ehrbar, E.; Zwahlen, J.; Martin, R.; Ziemer, J.; Connolly, W.; Rhodes, S. In *ST7-DRS Colloid Thruster System Development and Performance Summary*, Aiaa/asme/sae/asee Joint Propulsion Conference & Exhibit, 2008.
16. Liu, H.; Jiang, W.; Ning, Z. X.; Kai, C.; Zeng, M.; Cao, X. F.; Yu, D. R., Cusped field thruster using different propellants. *Wuli Xuebao/Acta Physica Sinica* **2018,** *67*, 145201.
17. Jenkins, M. G.; Krejci, D.; Lozano, P., CubeSat constellation management using Ionic Liquid Electrospray Propulsion. *Acta Astronautica* **2018**, S0094576517312511-.
18. Krejci, D.; Lozano, P., *Micro-machined ionic liquid electrospray thrusters for Cubesat applications*. 2017.
19. Zwahlen, J.; Hruby, V.; Campbell, C.; Demmons, N.; Ziemer, J. In *Flow control micro-valve for the ST7-DRS colloid thruster*, Aiaa/asme/sae/asee Joint Propulsion Conference & Exhibit, 2008.

20. Grustan-Gutierrez, E.; Gamero-Castaño, M., *Time-of-Flight Characterization of a Microfabricated Electrospray Thruster Emitter Array*. 2017.